22nd Computational Fluid Dynamics Conference
22-26 June 2015, Dallas, TX
AIAA 2015-2616

# Simulation of Boundary Layer Flows over Biofouled Surfaces

Jasim Sadique[1] Xiang I. A. Yang [2], Charles Meneveau[3] and Rajat Mittal[4]
*Department of Mechanical Engineering, The Johns Hopkins University, Baltimore, MD- 21210*

**This study presents a methodology for modeling a developing turbulent boundary layer flows over surfaces with large (macro-scale) rougness elements, with particular application to flow over bio-fouled surfaces. A sharp-interface immersed boundary method coupled with a wall model and large-eddy simulations is used to carry out accurate simulations of flow over such macro-bio-fouled surfaces. Simulation of flow over arrays of modeled barnacles with different barnacle density have been carried out, and results are presented on the effect of distribution density on the flow physics, and the drag on the surfaces. Furthermore, a surface containing roughness elements of two length-scales is compared to the single-scale case to illustrate the effect of having roughness elements of more than one scale.**

## Nomenclature

| | | |
|---|---|---|
| $A_f$ | = | frontal area of roughness elements |
| $A_p$ | = | plan area of roughness elements |
| $A_T$ | = | plan area of the surface |
| $C_D$ | = | drag co-efficient |
| $D$ | = | drag force acting on the surface |
| $d$ | = | zero-plane displacement |
| $h$ | = | roughness height |
| $k_s$ | = | "equivalent" sand roughness height |
| $U$ | = | mean strem-wise velocity |
| $u_\tau$ | = | friction velocity |
| $y_0$ | = | hydrodynamic roughness height |
| $\delta$ | = | boundary layer thickness |
| $\delta*$ | = | displacement thickness |
| $\kappa$ | = | von-Karman constant |
| $\lambda_f$ | = | solidity or frontal area index. Ratio of $A_f$ to $A_T$ |
| $\lambda p$ | = | planar area index. Ratio of $A_P$ to $A_T$ |

[1] Graduate Student, Department of Mechanical Engineering, The Johns Hopkins University, Student Member, AIAA
[2] Graduate Student, Department of Mechanical Engineering, The Johns Hopkins University, Student Member, AIAA
[3] Professor, Department of Mechanical Engineering, The Johns Hopkins University, Senior Member, AIAA.
[4] Professor, Department of Mechanical Engineering, The Johns Hopkins University, Associate Fellow, AIAA.

## I. Introduction

ACCURATE simulations of developing boundary layer flow over rough-surfaces is a challenging task - issues range from obtaining realistic inflow conditions to accurately resolving the wide range of length scales present in these flows. The present study is motivated by the need to understand the flow physics of rough surfaces in the context of bio-fouling. Bio-fouling is the phenomenon whereby various organisms attach themselves on to surfaces exposed to fluid, for example the hull of a ship, and is a serious concern for the maritime industry[1,2]. Other applications where the techniques presented here are applicable include insects and/or debris adhering to wind turbine blades and aircraft wings, pitted surfaces of ships, submarines, propellers and turbine blades and flow through pipes/conduits with large-scale rust buildup and other deposits. The present paper is concentrated on surfaces fouled by acorn barnacles, which are a common agent of bio-fouling[2,3]. The accretion of these hard-shell organisms lead to what is called hard or calcerous fouling. The shells of these orgainsms remain attached to the surface even after their death leading to sustained increases in drag and a higher fuel consumption. Gaining an understanding of flow over such surfaces can aid in estimating the timing and efficacy of remedial measures to combat bio-fouling. Direct numerical simulations (DNS) and wall resolved large eddy simulations (LES) are not feasible at realistic flow conditions due to computational constraints. In this study a sharp-interface immersed boundary method is used to represent the roughness elements on the computational grid. This is coupled with an LES that employs a wall-model for the near-wall stress. A rescaling/recycling method[4] modified for rough-wall boundary layers[5] is used to generate the inflow, which avoids the need to simulate the boundary layer transition from laminar to turbulent flow. Flows over idealized barnacle arrays are simulated with various roughness densities and explore the effect of roughness elements of multiple length scales on the flow.

## II. Methodology

Our in-house code Vicar3D is used to solve the 3-D Navier stokes equations in cartesian coordinates. This code is based on the sharp-interface immersed-boundary method[6,7]. The code employs a 3D ghost-cell methodology for imposing the boundary conditions on the solid boundary. Details of the implementation as well as validation for a variety of flow configurations is provided in Refs 6 and 7. The code uses a second-order accurate central-differecing scheme for the spatial derivaties and a second-order accurate fractional step scheme for the temporal integration. A

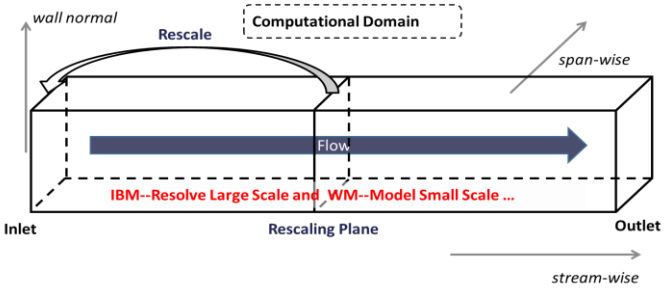


**Figure 1. Schematic of the solution methodology.**

global dynamic coefficient Vreman model is used for modelling the sub-grid stresses[8]. A newly developed integral wall model[9] is used for applying the boundary condition at the rough wall. The integral wall model includes non-equilibrium effects like flow acceleration pressure gradients etc., and gives better results when compared to an equilibrium wall model[10]. It is seen that such effects are important for flow over roughness elements as the integral wall model reacts to the local flow condition better[9]. Creating a correct inflow condition for a developing boundary layer is a difficult task especially for rough walls. Different methods are used in the literature – precurosor simulations, library generation or tripping the boundary layer using roughness elements. In this study a rescaling/recycling method following Lund et. al.[4] is used. This method was originally formulated for a developing boundary layer over a flat plate. Here a modified method[5], which takes into consideration the presence of the an inner roughness length scale, is used. This modified method along with the integral wall model is seen to perform well for the case of both smooth and rough walls[5,9]. The schematic of the solution methodology is shown in Fig 1. The immersed boundary methods resolves the large scales of the geometry while the wall model is used to model the effect of the small scales. The rescale plane is chosen in a region near the middle and the rescaled field is fed as an inlet to the flow.

## III. Results and Discussion

Acorn barnacles, which are the focus of the current study, are frequently represented as cones or frustum of cones[11]. Following this, conical frustums are used as an idealized representation of the barnacles. These geometries are created

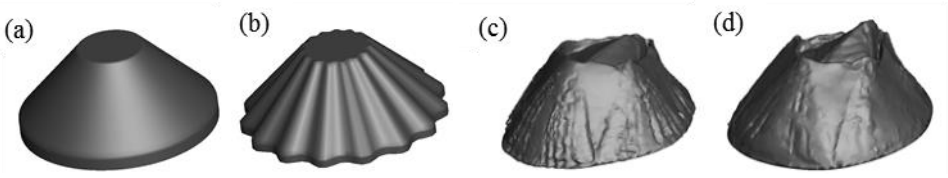


**Figure 2. Frustum model (a) without ridges (F1) and (b) with ridges (R1). Barnacle Geometries (c) B1 and (d) B2**

by extracting features from high-resolution scans of acorn barnacles. Figure 1 shows the two levels of frustum models created - F1 and R1 (1a and 1b) compared to two actual barnacle geometries B1 and B2 (3D barnacle scans provided by Dr. Michael Schultz of The Naval Academy). Tests were carried out at a moderate Reynolds number of 2000 with respect to the barnacle diameter and the free-stream velocity with a laminar boundary-layer as inlet which show the the essential flow features and the shedding strouhal number are similar for the idealized geometries when compared to that of the actual barnacles[12]. For these features both not much difference was seen between the two idealized models (F1 and R1). Thus for this study we choose to model the fouled surface as an array of conical frustum elements.

Similar to the case of a smooth flate the velocity profile for a flow over rough walls has an inertial layer governed by a log law[13]

$$\frac{U}{u_\tau} = \frac{1}{\kappa} log\left(\frac{y-d}{k_s}\right) + 8.5$$
$$\frac{U}{u_\tau} = \frac{1}{\kappa} log\left(\frac{y-d}{y_0}\right) \quad (1)$$

where $u_\tau = \sqrt{\frac{D}{\rho A_T}}$. $k_s$ and $y_0$ can both be used to characterize the roughness depending on the form of the equation used. An early study on different roughness elements was conducted by Schilchting[14] on spheres, cones and spherical segments. He found that for each type of roughness, $k_s/h$ (or equivalently $y_0/h$) increases with the frontal area ratio. This factor reaches a maximum for $\lambda_f$ around 0.2 and then decreases as the arrangement becomes dense and the elements start sheltering each other. The zero plane displacement ($d$) increases with $\lambda_f$ and approaches 1 as $\lambda_f$

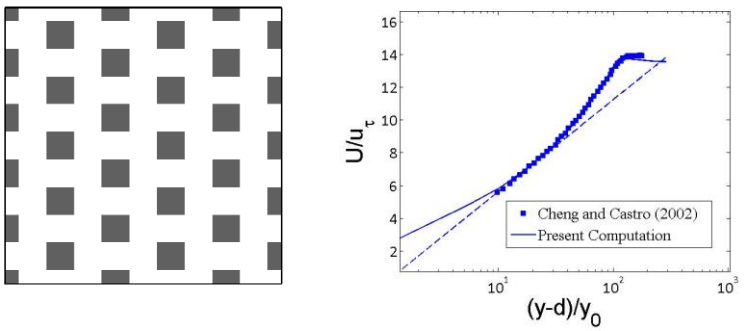


(a) (b)

**Figure 3. Geometry and comparison of computation with experiments.** (a) shows the top-view of a zoomed in view of the surface and (b) mean streamwise profile compared with the experiment[13].

approaches 1 in the case of cubic elements. Many of the detailed studies in recent literature for flow over three dimensional roughness elements deals with rectangular or cubic elements[15-18]. Our aim is to investigate the behavior of an array of idealized barnacle geometries and quantify their behavior with various arrangements and frontal areas. This study will concentrate on the frontal area ratios in the range of 0.02 to 0.1 for both aligned and staggered cases.

### A. Validation for flow over an array of cubes

Our solution methodology has been validated for various cases[9,19]. A further validation case is provided for flow over cubes of tightly packed arrays and a large roughness height (small δ/h)[20]. The case chosen has a frontal area density ($\lambda_f$) of 0.25 with a staggered arrangement. The Reynolds number is 12000 with respect to the free stream velocity and cube height. The measurements are made at a location where the boundary layer height δ/h =7 to match the experiment. Figure 3a shows the arrangement of the cubic elements. A grid size of 256 x 64 x 64 and a domain size of 64h x 8h x 8h is used. A reasonably good match with the experimental value for the mean profile (Fig 3b) is obtained. The comparison of the friction velocity and log-law parameters with the experiment are shown in Table 2. All the values match reasonably well with the experiment.

**Table 1: Comparison of friction velocity and log-law parameters**

| | $u_\tau$ | $d/h$ | $y_0/h$ |
|---|---|---|---|
| Present Simulation | 0.074 | .85 | .054 |
| Experiment[13] | 0.072 | .81 | .05 |

### B. Flow over Idealized Barnacle Arrays

For simulating the flow over idealized barnacle arrays an arrangement as shown in Fig 4 is used. The mesh size used is 256 x 64 x 64 and the simulations are carried out at a Reynolds number of $10^5$ based on the frustum base diameter and free stream velocity. The inlet boundary layer thickness is chosen to be δ/h = 4 and the Reynolds number based on friction velocity ($u_\tau$)and the boundary layer thickness is found to be in the range of 1 – 1.5 x $10^4$. Various configurations are obtained by varying the roughness element densities (varying $\lambda_f$) and the arrangment. For the frustum geometry chosen, the maximum possible $\lambda_f$ is 0.375 when the frustums are just touching each other. As mentoned earlier, this study looks at $\lambda_f$ in the range of 0.02-0.10. The simulations are run on the DOD HPC clusters and require about 250000-300000 CPU hours for each simulation. Figure 5a-c shows the instantaneous velocity field at the barnacle heights for aligned configuration at a value of $\lambda_f$ = 0.023 and 0.092. The simulations are carried out for around 75 flow-over times and statistics are collected after the first 35 flow-over times.

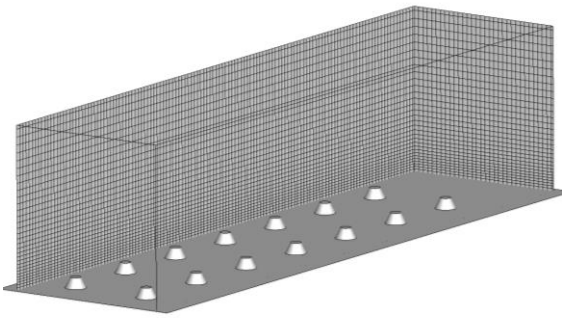

**Figure 4. The domain and the 256 x 64 x 64 grid (every other grid point is shown). The rough surface shown is an aligned array of $\lambda_f$ = 0.023**

The average drag is calculated for each row by averaging over time and in the span-wise direction and is used to calculate the friction velocity, Figure 6a shows the average friction velocity for each surface. It is seen that the friction velocity increases with $\lambda_f$ for both aligned and staggered arrangments from $\lambda_f$ = 0.023 to 0.092. Next a log-law is fitted to the averaged velocity profile using the average value of $u_\tau$ and the von-Karman coefficient $\kappa$ to calculate the hydrodynamic roughness height $y_0$ and the zero-plane displacement $d$ for each surface. Both $y_0$ and $d$ (Fig 6b-c) also increases with $\lambda_f$ . The values for the square and staggered arrangements remain similar for the three cases with some differences starting to become apparent at $\lambda_f$ = 0.092 case. At this point the staggered arrangement has higher values for $u_\tau$, $y_0$ and $d$. At smaller values of $\lambda_f$ the roughness elements are far apart enough that the interactions between the elements are not significant. This explains why at small values of $\lambda_f$ the effect of the roughness elements are not dependent on the arrangement but only on the value of $\lambda_f$. As $\lambda_f$ increases and the interactions between the elements become important and so the values can depend on the arrangement.

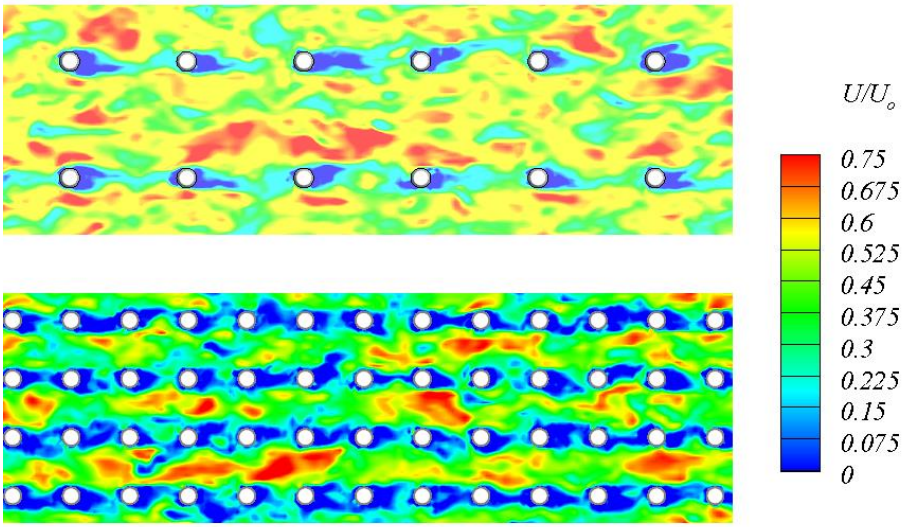


**Figure 5. Instantaneous contours of stremwise velocity for $\lambda_f$ = 0.023 and 0.092 at y/h = 0.625**

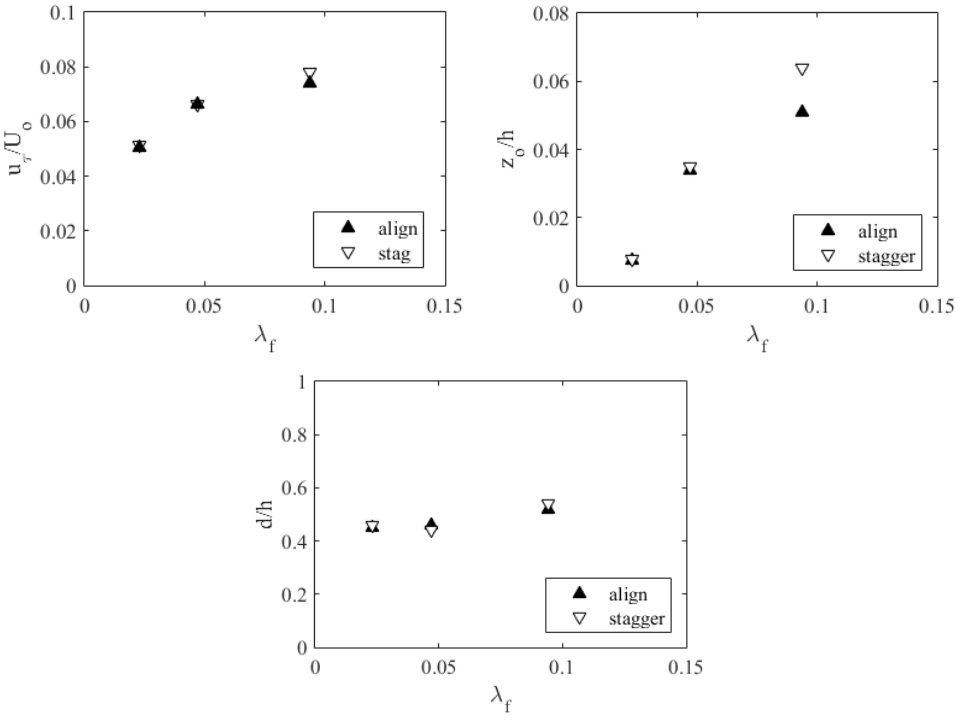


**Figure 6 Variation of (a) $u_\tau$ (b) $y_0$ and (c) d with $\lambda_f$ for both aligned and staggered cases**

Figure 7 shows the time averaged profiles of streamwise velocity for the case of frontal area ratio of 0.092 for both aligned and staggered arrangements. The contours are plotted at a location of y/h = 0.0625 from the base. For the aligned case, the flow is accelerated in between the columns while for the staggered case, this is broken up by the arrangement. Figure 8 shows the time averaged streamlines in the mid plane of a row of elements for the aligned cases with $\lambda_f = 0.092$ and $\lambda_f = 0.023$. For the higher $\lambda_f$ case, the flow below the roughness height is more isolated from the outer flow while the outer flow interacts more with the roughness elements for the lower $\lambda_f$ case. An illustration of this is the point P1 where the streamlines bifurcate is very near the apex for $\lambda_f = 0.092$ while for $\lambda_f = 0.023$. When that point is at the apex the inner flow is completely isolated from the surface and this is called a "*D* type roughness" or a "skimming" flow.

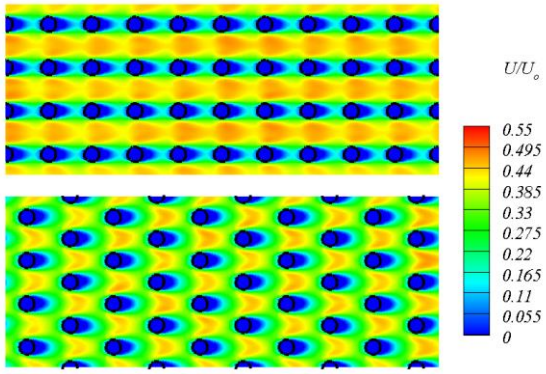


**Figure 7 Time averaged U velocity contours for $\lambda_f$ = 0.092 at y/h = 0.625. Top is aligned and bottom is staggered arrangement**

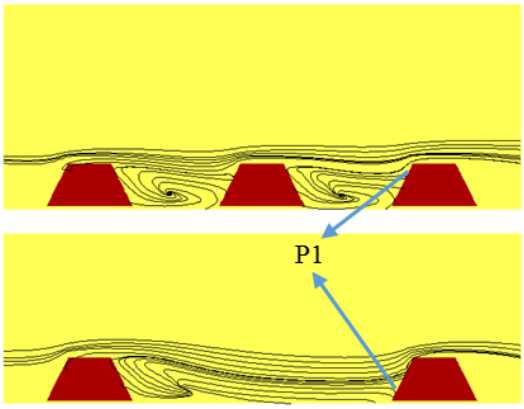


**Figure 8 Time averaged streamlines at the midplane for $\lambda_f$ = 0.092 and $\lambda_f$ = 0.023 aligned cases.**

### C. Multi-Scale Roughness Elements

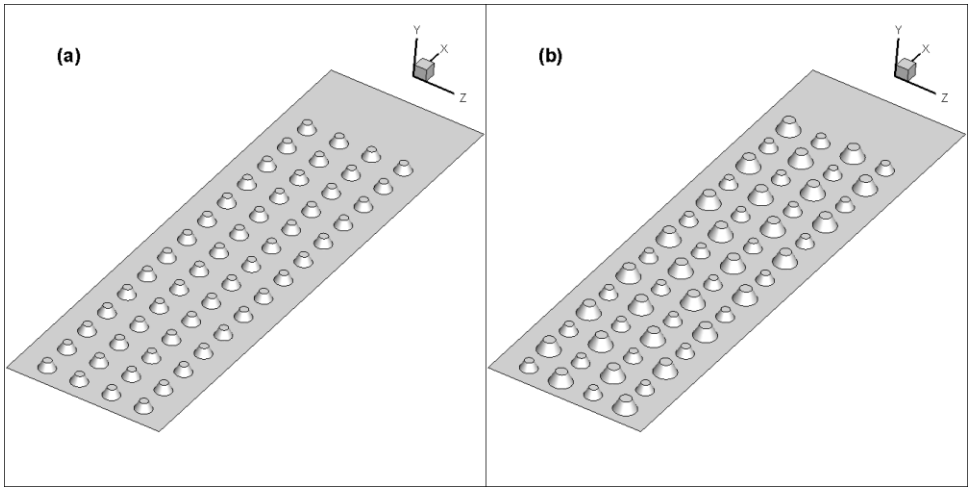


**Figure 9. (a) Single scale roughness and (b) Roughness at two-length scales obtained by replacing half of the roughness elements in (a)**

A realistic bio-fouled surface has roughnesses with a range of length scales. To replicate this feature surfaces with multiple scales has to be constructed. An example case of such a surface with two-scales (Figure 9b) is shown here

with elements of one scale being half of the other (as measured by the base and apex diameters and frustum height). The surface is created by scaling alternate elements of the single scale surface by a factor of 4/3 and 2/3 so that the mean height remains the same for the two surfaces. The frontal area however increases by a factor of 11%. Figure 10 shows the instantaneous vortex structures identified by the swirling strength criteria and colored by the pressure. The vortex structures are dominated by those created by the larger elements. Figure 11 shows the 2D streamlines for the two cases in the xz plane at the center-line of the roughness elements. The single scale case is same as that shown in Figure 7. For the two-scale case, the smaller scale roughness is isolated from the outer flow by the larger scale. Figure 12 shows the time-averaged velocity at $y/h_m$ = 0.625 for the two scale case, where $h_m$ is the mean height. The figure shows that the smaller scale is completely in the wake of the larger scale roughness element. The high velocity streaks are more confined and stronger than the single scale case due to the increased constriction caused by the large-scale roughness elements.

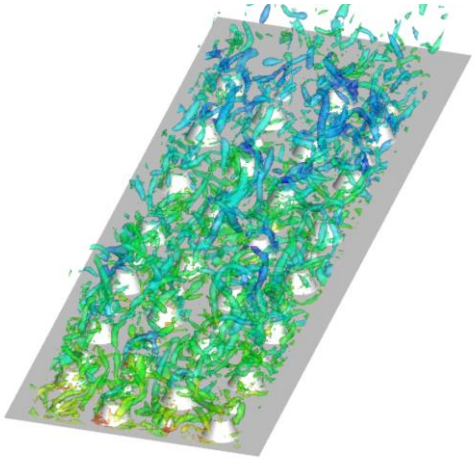

**Figure 10. instantaneous vortex structures colored by pressure for the two-scale case.**

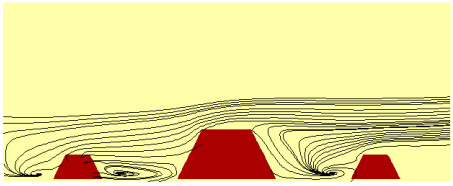

**Figure 11. Time-averaged 2D streamlines at the center plane for the two-scale simulations.**

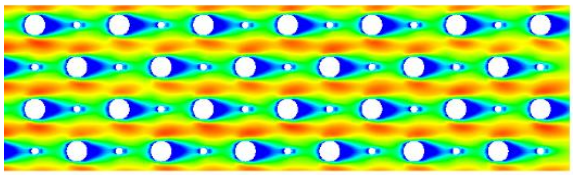

**Figure 12. Mean streamwise Velocity compared between the two-scale case at $y/h_m$ = 0.625**

### D. Conclusions

The simulation methodology developed here allows us to capture many of the properties of the turbulent flow over an array of idealized barnacle geometries. These simulations will help us parameterize the variation of the flow quanitites with surface properties like $\lambda_f$ and $\lambda_P$. Additional simulations will help in fully characterizing the behavior of the surface for a wide range of these parameters. For the range of frontal area ratios examined here, the the boundary layer parameters $y_0$, $d$ and the friction velocity $u_\tau$ all show an increase with the frontal area ratio, which is the expected behavior for the values of $\lambda_f$ studied here. Simulations at larger values of $\lambda_f$ should be investigated to identify the value of $\lambda_f$ at which $y_0$ and $u_\tau$ peaks, and their decreasing behavior beyond that value. It is also noted that the values of $y_0$, $d$ and $u_\tau$ are similar for both aligned and staggered arrangments for the frontal area ratios examined here. Finally, it is found that the preence of multi-scale roughness elements does have a considerable effect on the flow field, at least for the case examined here, and more simulations are required to parameterize the effect of different scale roughness elements on the flow field.

## Acknowledgments

This work is funded by ONR grant N00014-12-1-0582 monitored by Dr. Ronald Joslin. Computational resources for this work are provided via a Navy HPC Pathfinder award. We acknowledge collaboration and discussions with Dr. Michael Schultz of the US Naval Academy in this work.

## References

[1]Schultz, M.P., Bendick, J.A., Holm, E.R. and Hertel, W.M., "Economic Impact of Biofouling on a Naval Surface Ship", *Biofouling*, Vol. 27, No. 1 , 2011, pp. 87–98,.

[2]Woods Hole Oceanographic Institution, "Marine Fouling and its Prevention," United States Naval Institute, Annapolis MD, 1952.

[3]Otani M, Oumi T, Uwai S, Hanyuda T, Prabowo TRE, Yamaguchi T, Kawai H., "Occurrence and Diversity of Barnacles on International Ships Visiting Osaka Bay, Japan, and the Risk of introduction," *Biofouling*, Vol 23, No. 4, 2007, pp. 277–286.

[4]Lund, T. S., Wu, X., and Squires, K.D., "Generation of Turbulent Inflow Data for Spatially-Developing Boundary Layer Simulations," *Journal of Computional Physics*, 1998, Vol 140, No. 2, pp. 233-258.

[5]Yang, X.I.A, Meneveau C., "Recycling Inflow Method for Simulations of Spatially Evolving Turbulent Boundary Layers over Rough Surfaces," *Journal of Turbulence*, 2015, (under review).

[6]Mittal, R. Dong, H. Bozkurttas, M. Najjar, F.M. Vargas, A. Loebbecke, A.von, "A Versatile Sharp Interface Immersed Boundary Method for Incompressible Flows with Complex Boundaries*", Journal of Computational Physics*, Vol. 227, No. 10, 2008, pp. 4825-4852

[7]Seo, J.H. and Mittal, R., "A Sharp-Interface Immersed Boundary Method with Improved Mass Conservation and Reduced Spurious Pressure Oscillations", *Journal of Computional Physics*, Vol. 230, No. 19, 2011, pp. 7347-7363.

[8]You, D, Moin, P., "A Dynamic Global-Coefficient Subgrid-Scale Eddy-Viscosity Model for Large-Eddy Simulation in Complex Geometries," *Physics of Fluids*, Vol. 19, 2007, 065110

[9]Yang, X. I. A., Meneveau, C., Sadique, J., Mittal, R., "Integral Wall Model for Large Eddy Simulations of Wall-bounded Turbulent Flows," *Physics of Fluids*, Vol. 27, 2015, 025112

[10]Moeng C-H, 1984, "A Large-eddy Simulation Model for the Study of Planetary Boundary-layer Turbulence," *Journal of the Atmospheric Sciences*, Vol. 41, No. 13, 1984, pp. 2052-2062.

[11]Spivey, H.R., "Shell Morphometry in Barnacles: Quantification of Shape and Shape Change in Balanus," *Journal of Zoology*, Vol. 216, No. 2, 1988, pp. 265-294.

[12]Sadique, J., Yang, X.I.A., Meneveau, C., Schultz, M.P., and Mittal, R., "Flow over Barnacles: Characterization of Barnacle Geometry and Some Initial Flow Characteristics", *Bulletin of the American Physical Society* (abstract only), Vol. 58, 2013.

[13]Nikuradse J., "Strömungsgesetze in Rauhen Rohren," *VDI Forschungsheft 361*, 1933, (English translation "Laws of flow in rough pipes," *NACA TM 1292*, 1950)

[14]Schlichting, H., "Experimentelle Untersuchungen zum Rauhigkeitsproblem," *Ingenieur-Archiv*, Vol. 7, No. 1, 1936, pp. 1–34. (English translation "Experimental investigation of the problem of surface roughness," *NACA TM 823*, 1937)

[15]Xie, Z.T., Coceal, O., Castro, I.P., "Large-Eddy Simulation of Flows over Random Urban-like Obstacles," *Boundary-Layer Meteorology*, Vol. 129, No. 1, 2008, pp. 1–23

[16]Lee, J.H., Sung, H.J., Krogstad P.-Å, "Direct Numerical Simulation of the Turbulent Boundary Layer over a Cube-Roughened Wall,", *Journal of Fluid Mechanics*, Vol. 669, 2011, pp. 397-431

[17]Leonardi S., and Castro, I.P., "Channel Flow over Large Cube Roughness: A Direct Numerical Simulation Study", *Journal of Fluid Mechanics*, Vol. 651, 2010, 519-539.

[18]Hagishima, A., Tanimoto, J., Nagayama, K., Meno, S., "Aerodynamic Parameters of Regular Arrays of Rectangular Blocks with Various Geometries," *Boundary-Layer Meteorology*, Vol. 132, No. 2, 2009, pp. 315–337.

[19]Yang, X., Sadique, J., Mittal, R., and Meneveau, C., "Dynamic Immersed Boundary Method for Modeling of Turbulent Boundary Layers over Bio-Fouled Surfaces," *Bulletin of the American Physical Society* (abstract only), Vol. 58, 2013.

[20]Cheng, H., and Castro, I. P., "Near Wall Flow over Urban-Like Roughness", *Boundary-Layer Meteorology*, Vol. 104, No. 2, 2002, pp. 229–259.